

Laser Pattern-Write Crystallization of Amorphous SiC Alloys

C. PALMA¹ and C. SAPIA²

1.—University of “Roma Tre”, Department of Physics, Via della Vasca Navale, 84, 00146 Rome, Italy; and Istituto Nazionale Fisica della Materia (INFN). 2.—University of “Roma Tre”, Department of Electronics, Via della Vasca Navale, 84, 00146 Rome, Italy

The aim of this work is to investigate the cw-laser crystallization of amorphous $a\text{-Si}_{1-x}\text{C}_x$ alloys as a function of laser power and alloy composition. As the microRaman analysis reveals, many cases occur: in a silicon rich alloy ($x \approx 0.3$) we can obtain two crystalline phases, i.e. polycrystalline Si or polycrystalline C, depending on the laser energy density irradiated on the film. The presence of polycrystalline SiC is observed only in quasi-stoichiometric alloy ($x \approx 0.48$) in the cubic $\beta\text{-SiC}$ phase. The experiment has been performed with a laser pattern-writing system that permits simultaneous control of annealing energy and focused spot size. PC control allows several patterns to be traced on the same film.

Key words: Amorphous semiconductors, laser crystallization, thin films, direct laser write

INTRODUCTION

A strong interest is presently focused on laser crystallization of amorphous silicon films. This technique allows the fabrication of large-area electron circuits on glass substrate for use in electronics and photonic devices. For instance, at an industry level, this process has relevance for liquid crystal display technology.

The possibility of extending a similar technology to amorphous silicon-based compound semiconductors (in particular $a\text{-SiC}$) is very attractive but not trivial. The presence in the alloy of two (or, possibly, more) elements, with different thermal properties, is a reason why crystallization can be accompanied by phase segregation effects with the formation of several crystalline phases.

Here we present an investigation of the irradiation of $a\text{-Si}_{1-x}\text{C}_x$ alloy films, with carbon content in the range $x = 0.2\text{--}0.7$, performed with a cw Ar^+ ion laser and a pattern-write system. Silicon carbide (SiC) is considered an ideal material for high power/high temperature solid-state electronics as both a bulk semiconductor (hexagonal $\alpha\text{-SiC}$) and a heteroepitaxial layer on silicon (cubic $\beta\text{-SiC}$).¹

EXPERIMENT

The experiment we describe consists in irradiation of SiC films with a suitably driven laser beam.

The $a\text{-Si}_{1-x}\text{C}_x\text{:H}$ films, of about 1000 nm thickness, have been grown in a parallel plate glow-discharge by RF (13.56 MHz) decomposition of SiH_4/CH_4 gas mixture. The films were grown on glass substrates kept at 300°C at a total pressure of 1 torr and a constant $\text{SiH}_4 + \text{CH}_4$ flow rate of 10 sccm². Hydrogen dilution up to 90% was used. Elemental composition of these films was measured by electron microprobe analysis. We have obtained x values in the range of 0.1–0.7.

In the electron probe microanalyzer (EPMA), frequently referred to as electron microprobe, a focused electron beam is used to excite a small area on a specimen. Inelastic scattering events of several types result in a transfer of energy from the beam electrons to the atoms of the specimen, leading to the generation of characteristic x-rays. The analysis of the x-ray line yields compositional information with an accuracy of the order of 1–2% of the amount present for a given element.³

After deposition, samples have been irradiated with an Argon laser (at $\lambda = 514.5$ nm) with the aim of inducing crystallization by rapid thermal treatment. For a better control of the energy and the zone of

(Received October 18, 1999; accepted February 14, 2000)

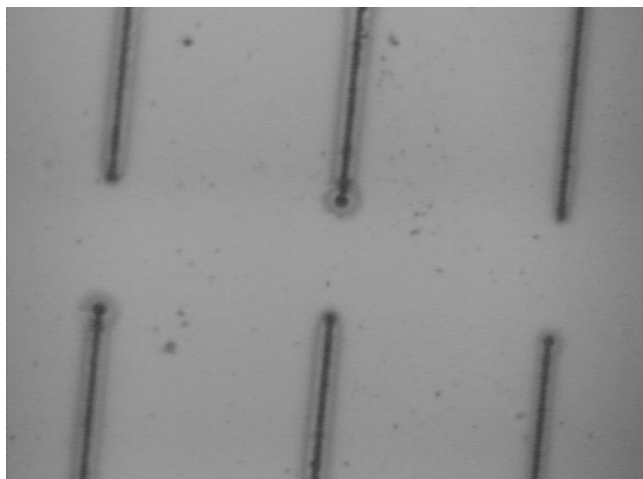


Fig. 1. Image at optical microscope (40x) of simple pattern on amorphous SiC film.

irradiation, we have developed a laser pattern-write system. Schematically, this system is a PC-controlled x-y translational stage with electro-optical autofocus and automatic exposure system. The aim was to “laser-write” crystalline patterns on the amorphous semiconductor with controlled and variable exposure.

As an example of a simple pattern, rows of less than 10 μm diameter have been written on a amorphous SiC film (Fig. 1), each row being distant 200 μm aside.

For a classification of crystallization effect, we have written a matrix of spots on the SiC film (Fig. 2). Each spot was obtained by different irradiation conditions. The most intensely irradiated row of spots (upper row in the Fig. 2) was laser-written with power of 1.5 W delivered by the laser, changing the irradiation time from 60 ms up to 240 ms in steps of 20 ms. The less intensely irradiated row was exposed to 5 mW and the same irradiation times.

The resulting energy densities were in the range 5×10^3 to $5 \times 10^6 \text{ J cm}^{-1}$. Due to heat diffusion, the spot diameters range from about 10 μm , for the less intensely irradiated spots to about double in the most intensely irradiated. Laser treatments were performed in air at room temperature.

The laser delivers a beam with a transverse Gaussian distribution of intensity. This distribution is maintained when the beam is focused, having undergone mainly propagation and focusing processes. Minor processes occurred along the optical path are reflection by the mirrors, absorption and partial obscurations by the lenses of the optical focusing system; these processes did not appreciably affect the shape of the distribution.

Local morphological changes of the film were monitored by scanning electron microscopy (SEM). Local structural and compositional characterization was performed with Raman microspectroscopy, using a Dilor spectrometer equipped with 633 nm HeNe excitation source. The system uses Olympus microfocusing optics, a single monochromator with an optical notch filter and CCD detection. The exciting light was focused down to a 1 μm spot size. Spectral resolution was 1 cm^{-1} .

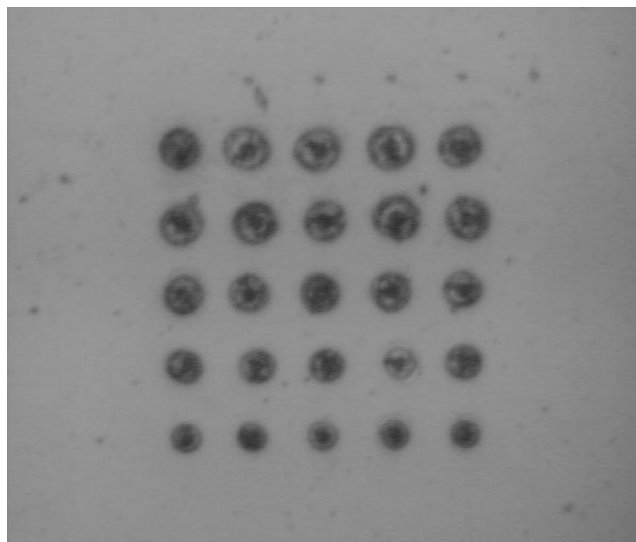


Fig. 2. Matrix of spots for the classification of crystallization energy. Image taken with optical microscope (40x)

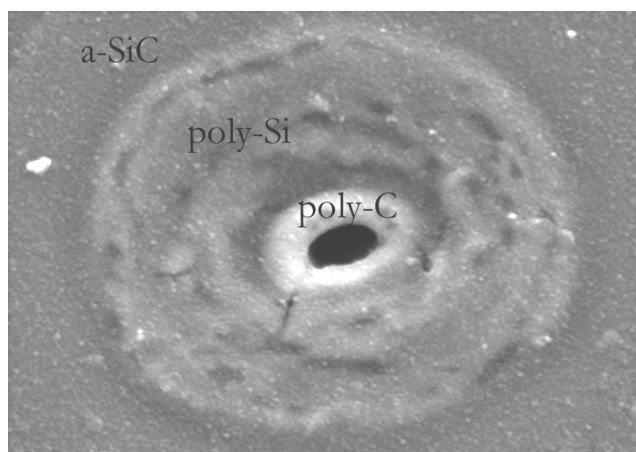


Fig 3. SEM image (10.000x) of a high-energy spot; circular region of different grey color.

Raman spectra offer a powerful method to gain information on material composition and structure, particularly when covalent solids are involved. In this case, phonon frequencies are strictly related to the nature of bonded atoms and phonon lineshapes depend on the order present in the solid. Therefore this technique is a good alternative to other well used techniques.⁴ Moreover, recent progresses of Raman spectrometers allow measurements with high lateral resolution (typically 1 μm) and high sensitivity (using single monochromators with notch filters and cooled detectors) to be done.

RESULTS AND DISCUSSION

The morphological analysis performed with SEM, shows that, at the highest energy delivered, the spots present an inner series of circular regions each having different grey color. These regions correspond to radial intervals where a different laser intensity was incident (because of the Gaussian distribution) and a different crystallization effect resulted, as the Ra-

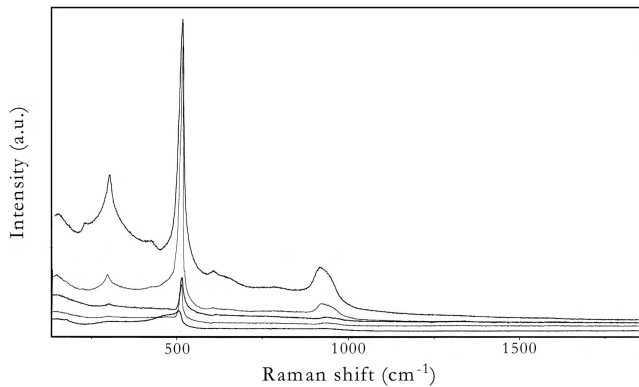


Fig. 4. MicroRaman spectra of selected irradiated spots on a-Si_{1-x}C_x sample ($x \approx 0.3$). Low energy density ($\approx 10^4 \text{ W cm}^{-2}$). Only the Si phonon line is enhanced in these spots.

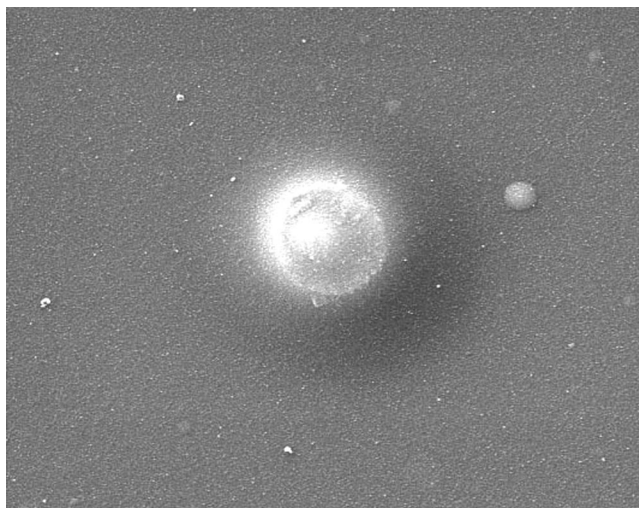


Fig. 5. Morphologically uniform crystallisation of polycrystalline Si obtained on a-Si_{1-x}C_x film ($x \approx 0.3$). SEM image (3000x) of low energy spot.

man spectroscopic analysis (1 μm lateral resolution) confirms.

Many different kinds of crystallization (illustrated with Figs. 3–9) are present. In particular, a central innermost black region is visible in Fig. 3 that corresponds to sublimation of the SiC alloy (probably with formation of gaseous SiO compound, since laser processing is accomplished in air).

The following region (low grey) presents Raman fingerprint of graphitization of carbon; the outer (high grey) of microcrystalline silicon.

This spatial separation depends on the Gaussian transverse profile of the beam that causes the annealing temperature to decrease with distance from the center of the spot. This, in turn, allows the different phase crystallization of SiC components: poly-C (high temperature) near the center, poly-Si (lower temperature) far from the center.

In another spots of the matrix illustrated in Fig. 2, we have obtained only one phase crystallization; poly-Si or poly-C.

Figure 4 shows Raman spectra of selected spots in which only the silicon TO phonon line (around 520 cm^{-1}) is present.⁵ These spots correspond to situations in

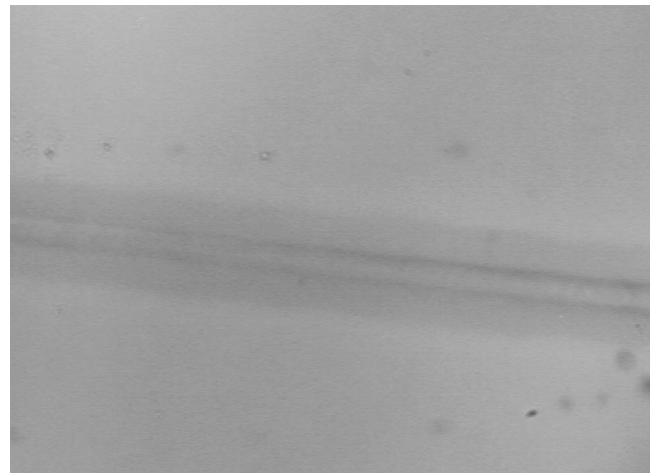


Fig. 6. Morphologically uniform crystallisation of polycrystalline Si obtained on a-Si_{1-x}C_x film ($x \approx 0.3$). Optical image (40x) of low energy line.

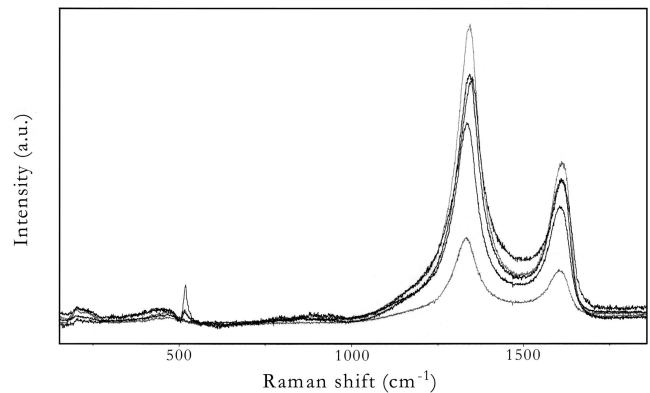


Fig. 7. MicroRaman spectra of selected irradiated spots on an a-Si_{1-x}C_x sample ($x \approx 0.3$). High energy density ($\approx 10^6 \text{ W cm}^{-2}$). The graphite phonon line is enhanced in spots of better quality of crystallisation.

which a lower energy has been delivered, ranging from 15 mJ to 40 mJ.

Among them, the better results are for the less exposed spots. In Fig. 5, a SEM image of one of these spots is presented. In this case, we observe a better morphological quality.

We also tried to obtain the same one-phase crystallization in other irradiation patterns. As an example, in Fig. 6 we present a crystallization pattern having a shape of a line. Here also a good morphological quality and uniformity of the line is observed.

These last features are more easily obtained in films with low concentration ($x \approx 0.3$) of C. These results are analogous to well known results of laser crystallization of amorphous silicon layer on glass substrate for fabricating large area electronic circuits;⁶ the effects already known for Si are extended to silicon rich alloys of amorphous SiC.

Figure 7 shows Raman spectra in which only the typical lines of graphite are present. Silicon spectral lines substantially disappear and broad bands arise at 1350 cm^{-1} and 1600 cm^{-1} .

These bands are characteristic of polycrystalline graphite.⁷ The lower frequency band (G band) corresponds to graphite TO phonon at the Brillouin zone

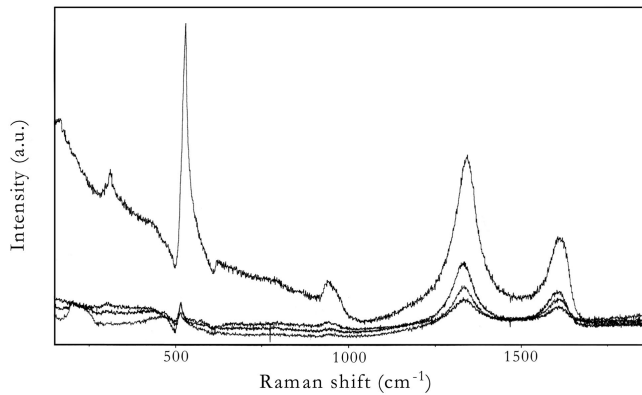


Fig. 8. MicroRaman spectra of selected irradiated spots on an $a\text{-Si}_{1-x}\text{C}_x$ sample ($x=0.3$). Intermediate energy density ($\approx 2.6 \times 10^5 \text{ W cm}^{-2}$). Both phonon lines, for Si and graphite, are enhanced.

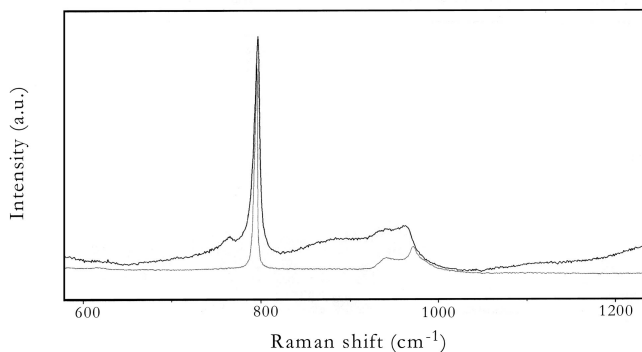


Fig. 9. MicroRaman spectra of selected irradiated spots ($\approx 8 \times 10^5 \text{ W cm}^{-2}$) on $a\text{-Si}_{1-x}\text{C}_x$ sample ($x = 0.46$). Typical $\beta\text{-SiC}$ phonon lines are enhanced in spots of better quality.

center; the other (D band) corresponds to a maximum of graphite phonon density, located at Brillouin zone boundary and made Raman active by disorder effect. It is worth noticing that this effect is the same obtained in highest energy spots in the zone near the center (see Fig. 3).

Figure 8 shows Raman spectra in which both the typical lines of crystalline Si and the D and G doublet of graphite are present, meaning that a simultaneous crystallization of the two species has been obtained.

These last results lead to the conclusion that crystallization of compound semiconductors is not trivial, since it can be accompanied by phase segregation effects. Therefore, strict experimental conditions are required, as is reported for the cases of annealing compound semiconductors.⁸

Figure 9 shows Raman spectra of selected spots in which the typical fingerprint of crystalline SiC appears. Sharp Raman bands around 790 cm^{-1} were observed together with weaker and broader features at $900\text{--}1000 \text{ cm}^{-1}$ range.

By comparison with Raman spectra of reference

crystalline silicon carbide polytypes, these spectra demonstrate the production of cubic SiC ($\beta\text{-SiC}$) crystalline phase.

The Raman analysis suggests that our laser crystallization technique preferentially promotes the formation of cubic polytypes ($\beta\text{-SiC}$), while the spectral signature of hexagonal phases $\alpha\text{-SiC}$ (lines at 970 cm^{-1}) is not observed in this situation.

We note that the crystalline phase of SiC, without the phenomenon of segregation, has been obtained only for particular high energy densities and particular film compositions ($x = 0.48$; near to stoichiometric ratio).

CONCLUSION

In conclusion, we have experimentally shown that irradiation of amorphous $a\text{-Si}_{1-x}\text{C}_x$ alloys with a cw-laser can produce a variety of crystalline results, depending on the laser energy delivered and on the carbon concentration in the film. The controlled formation of SiC crystalline phase is possible only when the alloy composition is in the quasi-stoichiometric range $x \approx 0.4\text{--}0.5$.

The morphological quality of the SiC crystallized pattern can be improved by a proper shaping of the laser beam that can lead to delivery of a more flattened intensity distribution (with respect to the Gaussian) on the film.

The pattern-write system allows control of the zone of crystallization and of the energy density. This permits pre-established patterns of crystallization and local variation of the crystallized product.

Crystallization of $a\text{-SiC}$ with such a variety of products can originate a number of electronic and photonic devices.^{9,10}

ACKNOWLEDGEMENTS

This work has been developed with contribution from Ente Nazionale Energie Alternative (ENEA).

REFERENCES

1. V.E. Chelnokov, A.L. Syrkin, and V.A. Dmitriev, *Diamond Relat. Mater.* 6, 1448 (1997).
2. G. De Cesare, F. Galluzzi, G. Guattari, G. Leo, and G. Vincenzoni, *Diamond Relat. Mater.* 2, 773 (1993).
3. Goldstein, Newbury, Echlin, Joy, Roring, Lyman, Fiori, and Lifshin, *Scanning Electron Microscopy and X-Ray Microanalysis* (New York: Plenum Press, 1992).
4. G. De Cesare et al., *Appl. Surf. Sci.* 106, 193 (1996).
5. J.S. Lannin, L.J. Pilione, S.T. Kshirsagar, R. Messier, and R.C. Ross, *Phys. Rev. B* 26, 3505 (1982).
6. T. Sameshima, *Mater. Sci. Eng. B* 45, 186 (1997).
7. N. Wada, P.J. Gaczi, and S.A. Solin, *J. Non-Crystall. Solid* 35, 543 (1980).
8. G. Vitali, *Jpn. J. Appl. Phys.* 31, 2049 (1992).
9. G.L. Harris and C.Y.-W. Wang, editors, *Proc. Amorphous and Crystalline Silicon Carbide* (Washington D.C.: Springer Verlag, 1987).
10. *J. Electron. Mater.* Special Issue on 38th EMC, 3 (1997).